Systematic Reduction of Peak and Average Emissions of Power Electronic Converters by the Application of Spread Spectrum

Andreas Bendicks, *Student Member, IEEE*, Stephan Frei, *Senior Member, IEEE*, Norbert Hees, and Marc Wiegand

***Abstract*—This paper deals with the application of spread spectrum techniques on power electronic converters to reduce electromagnetic disturbances. These techniques aim for a spreading of the harmonics in a frequency domain in order to distribute the power over a wider frequency range. By doing so, the levels of the harmonics drop. In this paper, both peak and average detector measurements are considered. It is shown that different parameters are required to minimize either peak or average emissions. The reduction of peak and/or average emissions is mathematically described for a sine wave as a harmonic of pulse width modulation signals. These spread harmonics overlap for high orders and/or high-frequency variations. It is shown that this effect is a limiting factor for spread spectrum in practical applications. The resulting maximum achievable reduction is analyzed. From these results, parametrization strategies are derived to fulfill specific requirements. In test setups, the precision of the proposed parametrization strategies is demonstrated. Additionally, it is shown that the results for peak measurements can also be applied to quasi-peak measurements.**

***Index Terms*—Average detector, electromagnetic interferences (EMI), parametrization, peak detector, power electronics, quasi-peak detector, spread spectrum.**

I. Introduction

Power electronic converters can be sources for high electromagnetic interferences (EMI) in, e.g., automotive systems. To prevent the disturbance of communication systems or, e.g., safety critical sensor systems, the emissions are limited by legal regulations [1] that are based on international standards [2]. Vehicle manufacturers often set even lower limits to ensure a high performance of even very sensitive wireless systems.

Due to the demand for increasing power densities of the individual converters, effective solutions for EMI reduction are a necessity. The different passive strategies like filters and shields suffer from additional weight, space, and cost. These strategies reduce the EMI that has been already caused by the power electronic system. Spread spectrum techniques, on the other hand, are an active solution that partially prevents the occurrence of disturbances. Normally, power electronic converters operate at a fixed switching frequency causing distinctive harmonics in the frequency spectrum. By the application of spread spectrum, the switching frequency is varied over time. So, the power of the harmonics is distributed in the frequency spectrum and the respective values drop.

There are many different works, e.g., [3]–[9], analyzing the impact of spread spectrum on the peak emissions of clocked systems. In [5], a holistic study is done on spread spectrum in dc-to-dc converters. Aspects include peak EMI reduction, voltage ripple, and efficiency drop. The influences of deterministic [3], [4] and randomized [8], [9] modulation schemes and their parameters are discussed and compared. In [5]–[7], the same optimum modulation time (slightly higher than 1/RBW (resolution bandwidth)) is found for the minimization of the peak emissions.

Furthermore, in [10] and [11], it has been shown that spread spectrum has no critical effect on the efficiency of power electronic converters if nonlinear terms are not dominant. Spread spectrum for interleaved parallel converters is investigated and advanced in [12]–[14].

There are many publications, e.g., [15]–[17], discussing spread spectrum for pulse width modulation (PWM) inverter systems. In [15], different modulation schemes are compared. In [16], two different modulation schemes are proposed: 1) spread spectrum with a uniform distribution; or 2) spread spectrum with a biased distribution that takes the impedance of the system into account. In [17], an optimized modulation scheme is derived that suppresses both acoustic and electromagnetic noise.

In [18], the parameters of spread spectrum are elaborated in such way that specific frequency components are suppressed. For cellular and wireless subsystems, a method is described on how to notch the spread spectrum for specific radio frequencies in [19]. In [20], the impact of different modulation schemes on the audio quality of class-D audio amplifiers is investigated. In [21], it is shown that spread spectrum has a positive effect on frequency modulation (FM) radio as a typical EMI sink.

In [22], a comparative analysis is done on the impact of spread spectrum on peak and average emissions of dc-to-dc converters for ramp modulation. It has been shown that different modulations times must be set if either peak or average emissions shall be reduced.

Manuscript received August 21, 2017; revised October 27, 2017; accepted November 5, 2017. Date of publication December 19, 2017; date of current version May 29, 2018. *(Corresponding author: Andreas Bendicks.)*

A. Bendicks and S. Frei are with the On-Board Systems Lab, TU Dortmund University, Dortmund 44227, Germany (e-mail: andreas.bendicks@tu-dortmund.de; stephan.frei@tu-dortmund.de).

N. Hees and M. Wiegand are with Leopold Kostal GmbH & Co. KG, Lüdenscheid 58513, Germany (e-mail: n.hees@kostal.com; m.wiegand@kostal.com).

Color versions of one or more of the figures in this paper are available online at http://ieeexplore.ieee.org.

Digital Object Identifier 10.1109/TEMC.2017.2777996

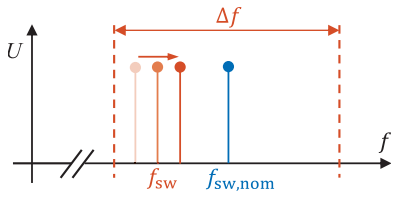

Fig. 1. Principle of spread spectrum.

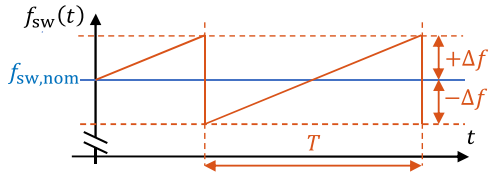

Fig. 2. Ramp modulation scheme.

This work contributes a proceeding analysis on the interdependences between peak and average emissions for a ramp modulation. To derive the maximum achievable reduction, sine waves are investigated at first. These results are transferred to PWM signals. In a further analysis, it is shown that overlaps between spread harmonics reduce the effectivity of spread spectrum. From these insights, systematic strategies are derived on how to determine the parameters of spread spectrum in order to fulfill specific requirements.

At first, the basics of spread spectrum technique and spectrum analyzers are repeated. Afterward, the influence of spread spectrum on the peak and average emissions is analyzed in detail. The theoretical results are integrated to parametrization schemes for practical applications. As a demonstration, the presented methods are applied to different test systems and are validated. Furthermore, it is shown that the results for the peak detector can be transferred to the quasi-peak detector. A conclusion closes the work.

II. Spread Spectrum

In Fig. 1, the basic principle of spread spectrum on power electronic converters is illustrated. In an unmodulated PWM signal, there is a fixed fundamental wave $f_{\mathrm{sw,nom}}$. By the application of spread spectrum, the harmonic $f_{\mathrm{sw}}(t)$ is shifted in the frequency spectrum over time. The range for the variation is $\pm\Delta f$ around the nominal switching frequency $f_{\mathrm{sw,nom}}$.

There are many different frequency modulation schemes including, e.g., sinusoidal [3], cubic [4], triangular [4], randomized [8], and pseudorandomized waveforms [9]. As stated in [5], triangular modulation is simple, effective, and most common. As theoretically derived in [6] and practically shown in [7], the related ramp modulation is even more effective. Hence, a linear ramp modulation is investigated in this paper. This scheme is shown in Fig. 2. T is the modulation time.

III. Spectrum Analyzer Basics

For the analysis of emissions, a spectrum analyzer or measuring receiver can be used. As the general behavior is similar, only the spectrum analyzer is considered here. In Fig. 3, the basic structure is depicted [5]. A central component is the band-pass filter with the resolution bandwidth RBW. As the spectrum analyzer shall measure a wide frequency band and the band-pass filter is fixed to its center frequency (the intermediate frequency), the input signal needs to be shifted in the frequency domain by a mixer and a local oscillator. Behind the RBW filter, there is an envelope detector to find the envelope of the signal. The resulting signal is low-pass filtered with the video bandwidth to reduce noise on the instrument screen. At last, there is a detector block to evaluate the signal. In this paper, the focus lies on two important detectors: peak and average. The peak detector searches for the highest value of the envelope of the signal. The average detector takes the mean of the envelope over time.

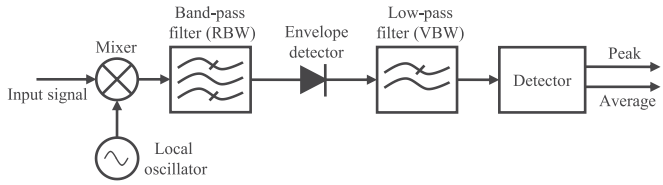

Fig. 3. Basic structure of a spectrum analyzer [5].

For the analysis in this paper, frequencies below 30 MHz are investigated. Therefore a RBW of 9 kHz (at –6 dB) is used that demands a minimum measurement time of 50 ms [2]. According to [2], the measurement time T_{meas} must be larger than the pulse repetition time that equals the modulation time T for spread spectrum. As the longest considered modulation time T in this work equals 10 ms, the minimum measurement time is sufficient. So, the sweep time of the spectrum analyzer is set to $T_{\mathrm{sweep}} = N \cdot T_{\mathrm{meas}}$ where N is the number of the considered frequency points.

IV. Minimizing Peak Emissions

In this section, the influence of spread spectrum on peak emissions is discussed. First, the optimum modulation time is determined. Second, the reduction for single sine waves is analyzed. Third, the results are transferred to PWM signals. Finally, a parametrization strategy is presented on how to apply the results. As an example, spread spectrum is applied to a burst signal.

A. Optimum Modulation Time

To find the optimum modulation time, a parameter study on the frequency deviation Δf and the modulation time T is performed. In this study, a single sine wave (representing one harmonic of a PWM signal) with an amplitude of 1 V and a nominal frequency of 250 kHz is utilized. In Fig. 4, the measured peak emissions are illustrated.

If there is no modulation ($\Delta f = 0$ kHz), the peak value is approximately 117 dBµV (RMS value of the sine wave). The higher the value of the frequency variation Δf, the further the values of the peak drop. This is due to the fact that the power of the harmonic is spread over a wider frequency range. Interestingly, for all considered frequency variations, there is a dependence on the modulation time T. There is a minimum for a modulation time of $T \approx 100$ µs that is slightly lower

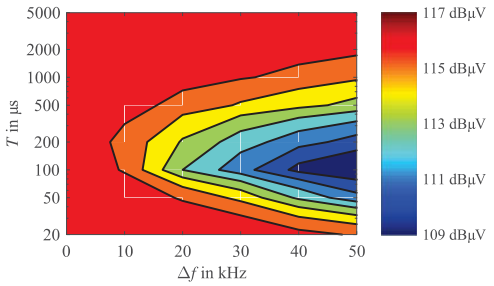

Fig. 4. Parameter study on peak emissions, RBW = 9 kHz.

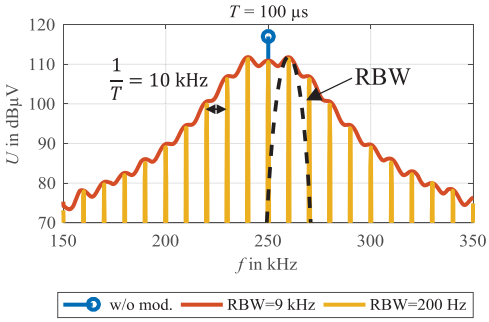

Fig. 5. Peak spectra for an ideal T and $\Delta f = 25$ kHz.

than $1/\mathrm{RBW} = 1/9\,\mathrm{kHz} \approx 111.1\,\mu\mathrm{s}$. This effect has also been shown in [5]–[7], and [22].

For explanation, the ideal case is investigated further in the frequency spectrum (see Fig. 5). It can be seen that the unmodulated signal has a peak value of 117 dBµV. Due to the modulation, the harmonic is spread over a wide frequency range. In the measurement with a RBW of 200 Hz, discrete subharmonics with a spacing of $1/T = 1/100\,\mu\mathrm{s} \approx 10$ kHz become visible [25]. If a RBW of 9 kHz is used, there are maximum values at 240 and 260 kHz. Under consideration of the RBW at 260 kHz, it is obvious that there is basically only one subharmonic having a significant influence on the peak value. So, a peak value of approximately 112 dBµV results. [22]

A further reduction of the modulation time would result in fewer subharmonics with more spacing. Still, only one subharmonic would contribute to the RBW. But, due to the fewer subharmonics, the power is not distributed as much. Therefore, a higher peak value results. [22]

An increase of the modulation time would cause more subharmonics with less spacing and even lower individual peak values as the power is distributed to more frequencies. Nevertheless, due to the reduced spacing, there are multiple subharmonics contributing in the RBW. Therefore, the peak value increases. [22]

So, to minimize the emissions measured with the peak detector, the modulation time T should be slightly lower than 1/RBW:

$$T \lesssim 1/\mathrm{RBW}. \tag{1}$$

For a RBW of 9 kHz, a modulation time T of 100 µs results. It is notable that the corresponding frequency of 10 kHz is in the audible spectrum. So, an annoying whistle may occur [4]. The frequency variation Δf should be as large as possible to minimize the measured peak emissions.

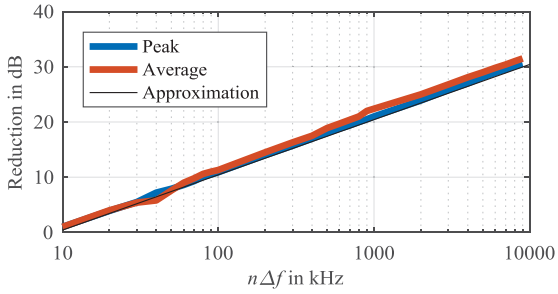

Fig. 6. Reduction of the peak and average emissions for RBW = 9 kHz and $T = 100$ µs.

B. Reduction for a Single Sine Wave

In this section, the reduction for single sine waves is analyzed as representation of harmonics of PWM signals. As the peak emissions shall be minimized, the ideal modulation time T of 100 µs is applied. In Fig. 6, the reduction of the peak and average emissions is illustrated in the dependence of the frequency variation $n\Delta f$ where n is the order of the harmonic and Δf is the frequency variation of the fundamental wave. So, $n\Delta f$ is the frequency variation of the nth harmonic.

It is assumed that the considered sine wave is the fundamental wave of a PWM signal, so n equals 1. A nominal frequency of 10 MHz is used. Of course, the sine wave cannot be modulated down to 0 Hz. So, the possible frequency modulation is limited by the nominal frequency: $\Delta f_{\max} \lesssim f_{\mathrm{sw,nom}}$. Reasonably, the reduction of the emission increases with the frequency variation as the harmonic's power is spread to a wider frequency range. Interestingly, peak and average emissions are reduced equally.

Next, the relationship found in Fig. 6 is analyzed. The spectrum of a single chirp may be described by [24]

$$|S(f)| = \sqrt{\frac{T}{4 \cdot n\Delta f}} \cdot \sqrt{[C(X_2) - C(X_1)]^2 + [S(X_2) - S(X_1)]^2} \tag{2}$$

$$\text{with } X_1 = -2(f - f_{\mathrm{sw,nom}}) \cdot \sqrt{\frac{T}{4n\Delta f}} - \sqrt{T \cdot n\Delta f} \tag{3}$$

$$\text{and } X_2 = -2(f - f_{\mathrm{sw,nom}}) \cdot \sqrt{\frac{T}{4n\Delta f}} + \sqrt{T \cdot n\Delta f} \tag{4}$$

where $C(x)$ and $S(x)$ are the solutions of the respective cosine and sine Fresnel integrals. To find the resulting voltage, the spectrum has to be weighted by the original peak value U_{Peak}. Additionally, as the chirp is not singular but repeated with T, the following spectrum results:

$$|U(f)| = \sqrt{\frac{T}{4 \cdot n\Delta f}} \cdot \sqrt{[C(X_2) - C(X_1)]^2 + [S(X_2) - S(X_1)]^2} \cdot U_{\mathrm{Peak}} \cdot \frac{1}{T} \sum_{k \in \mathbb{Z}} \delta(f - k \cdot T). \tag{5}$$

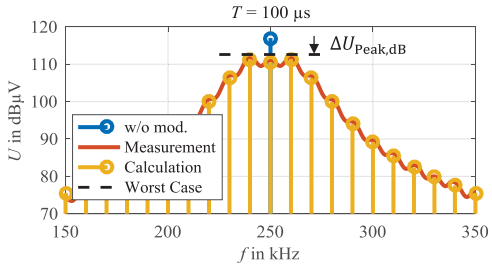

Fig. 7. Calculated and measured spectra.

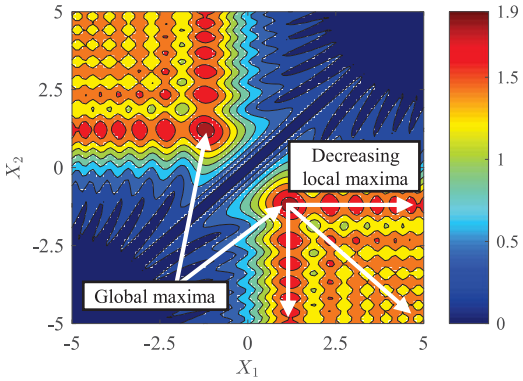

Fig. 8. Graphical representation of $\sqrt{[C(X_2)-C(X_1)]^2+[S(X_2)-S(X_1)]^2}$.

In Fig. 7, a comparison between the measured and calculated spectra is depicted. There is a high agreement confirming the calculation.

Next, the maximum value of the spectrum $|U(f)|$ must be determined. Therefore, the term

$$\sqrt{[C(X_2)-C(X_1)]^2+[S(X_2)-S(X_1)]^2}$$

is investigated. In the graphical representation in Fig. 8, there are two global maxima at approximately (–1.2, 1.2) and (1.2, –1.2) with values close to 1.90. The numerous local maxima decrease with an increasing distance from the global maxima. So, the investigated term may be approximated by

$$\sqrt{[C(X_2)-C(X_1)]^2+[S(X_2)-S(X_1)]^2} < 1.90\,. \quad (6)$$

With (6), (5) may be simplified to

$$|U(f)| < U_{\mathrm{Peak}} \cdot 1.90 \cdot \sqrt{\frac{1}{4 \cdot n\Delta f \cdot T}} = U_{\mathrm{Peak}} \cdot 0.95 \cdot \sqrt{\frac{1}{n\Delta f \cdot T}}. \quad (7)$$

So, the worst case of the subharmonics may be calculated by

$$U_{\mathrm{level}} = U_{\mathrm{Peak}} \cdot 0.95 \cdot \sqrt{1/(n\Delta f \cdot T)} \quad (8)$$

$$U_{\mathrm{level,dB}} \approx U_{\mathrm{Peak}} - 20\,\mathrm{dB} \cdot \log_{10}\left(1.05 \cdot \sqrt{n\Delta f \cdot T}\right). \quad (9)$$

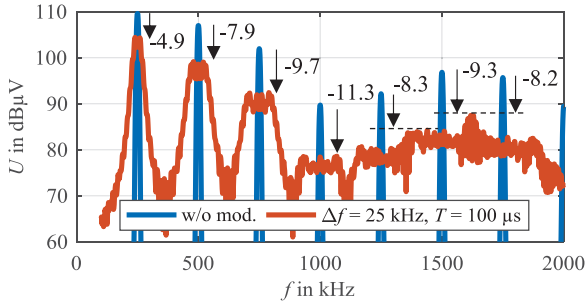

Fig. 9. Exemplary spectra of PWM signals, $f_{\mathrm{sw,nom}} = 250\,\mathrm{kHz}$, $d = 77\%$.

TABLE I
PEAK REDUCTIONS IN THE EXEMPLARY SPECTRA

Harmonic	1	2	3	4	5	6	7
Δf/kHz	25	50	75	100	125	150	175
$\Delta U_{\mathrm{Peak,dB,meas}}$/dB	4.9	7.9	9.7	11.3	8.3	9.3	8.2
$\Delta U_{\mathrm{Peak,dB,calc}}$/dB	4.4	7.4	9.2	10.4	11.4	12.2	12.9

Hence, the reduction is described by

$$\Delta U_{\mathrm{Peak,dB}} = 20\,\mathrm{dB} \cdot \log_{10}\left(1.05 \cdot \sqrt{n\Delta f \cdot T}\right). \quad (10)$$

This approximation is depicted in Fig. 6. There is a good agreement between calculation and measurement.

C. Reduction for a PWM Signal

Next, this result is applied to a PWM signal. There is a nominal switching frequency of 250 kHz and a frequency variation of 25 kHz for the fundamental wave. Both nominal frequency and frequency variation are proportionally increased with the order of the harmonic [23]. Therefore, the frequency variation of each harmonic n may be calculated by $n\Delta f$. As the frequency variation increases for each subsequent harmonic, the mitigation of the peak emissions increases in comparison to the fundamental wave. This effect can be seen in the spectra in Fig. 9. Table I shows a comparison between the calculated (10) and measured peak reductions of the harmonics.

Obviously, the highest reduction is achieved for the fourth harmonic. For higher harmonics, the reduction diminishes. This is due to the fact that the frequency bands of the harmonics overlap. In this case, a portion of other harmonics' power contributes to the power of the considered harmonic. Because of this, the reduction according to $\Delta U_{\mathrm{Peak,dB}}(n\Delta f)$ is mitigated for higher harmonics. This effect occurs for the first time if the upspread of the nth harmonic and the downspread of the $(n+1)$th harmonic overlap:

$$n\Delta f + (n+1)\,\Delta f \geq f_{\mathrm{sw,nom}}. \quad (11)$$

This formula results in the first harmonic n_{ovlp} that is affected by an overlap

$$n_{\mathrm{ovlp}} = \mathrm{ceil}\left(\frac{f_{\mathrm{sw,nom}}}{2\Delta f} - \frac{1}{2}\right). \quad (12)$$

In Fig. 9, it can be seen that the first overlap occurs for $n_{\mathrm{ovlp}} = 5$. For this and the subsequent harmonics, the reduction stagnates. So, for PWM signals, $\Delta U_{\mathrm{Peak,dB}}(n\Delta f)$ has to be specified as

$$\Delta U_{\mathrm{Peak,dB}}\left(n\Delta f\right) = 20\,\mathrm{dB}\cdot\log_{10}\left(1.05\cdot\sqrt{n\Delta f\cdot T}\right) \quad \text{for } n < n_{\mathrm{ovlp}} \tag{13}$$

$$\Delta U_{\mathrm{Peak,dB}}\left(n\Delta f\right) < 20\,\mathrm{dB}\cdot\log_{10}\left(1.05\cdot\sqrt{n_{\mathrm{ovlp}}\Delta f\cdot T}\right) \quad \text{for } n \geq n_{\mathrm{ovlp}} \tag{14}$$

with n_{ovlp} as stated above. So, the peak values are minimized for the last harmonic before an overlap occurs. To achieve the highest reduction possible for a specific harmonic n_{x}, the boundary to an overlap is aimed for:

$$n_{\mathrm{x}}\Delta f_{\max} + \left(n_{\mathrm{x}}+1\right)\Delta f_{\max} = f_{\mathrm{sw,nom}}$$

$$\Rightarrow \Delta f_{\max}\left(n_{\mathrm{x}}\right) = \frac{f_{\mathrm{sw,nom}}}{2n_{\mathrm{x}}+1}. \tag{15}$$

Therefore, the maximum achievable reduction may be calculated by

$$\Delta U_{\mathrm{Peak,dB,max}}\left(n_{\mathrm{x}}\Delta f_{\max}\left(n_{\mathrm{x}}\right)\right) = 20\,\mathrm{dB}\cdot\log_{10}\left(1.05\cdot\sqrt{n_{\mathrm{x}}\Delta f_{\max}\left(n_{\mathrm{x}}\right)\cdot T}\right). \tag{16}$$

D. Systematic Selection of Spread Spectrum Parameters

In this section, a systematic parametrization of spread spectrum for specific requirements is presented. In practice, there is often the problem that single harmonics violate the respective peak and/or average emissions. This parametrization strategy helps to find the right parameters to reduce the levels of critical harmonics below the given limits. This strategy has two use cases.

1) The peak emissions must be reduced.
2) The peak and average emissions must be reduced.

If only a reduction of the average emissions is necessary, the parametrization strategy presented in Section V-D can be applied.

For demonstration, a burst mode signal is considered. This signal consists of 1-ms-long-pulse packages that are repeated every 10 ms. Each package consists of trapezoidal pulses with a nominal switching frequency of 1 MHz, a duty cycle of 50%, and an amplitude of 100 $\mathrm{mV_{pp}}$. The signal is produced by an arbitrary waveform generator (Tektronix AFG3101). The spectra in the AM range (RBW of 9 kHz) and the class 1 voltage limit are depicted in Fig. 10. Obviously, both peak and average emissions are above the limit. The proposed parametrization strategy for spread spectrum consists of the following steps.

1) The modulation time is set according to (1). As AM with its RBW of 9 kHz is considered, a modulation time T of 100 µs results.
2) Next, the critical harmonic n_{x} has to be identified. If there are multiple critical harmonics, note that every harmonic before n_{x} is reduced less. All harmonics after n_{x} are still reduced but not as much as the harmonic n_{x}. In the example, the critical harmonic is the fundamental wave: $n_{\mathrm{x}} = 1$. To fulfill the requirements, peak and average have to be reduced by approximately 7 dB.
3) The maximum frequency variation without overlaps in the harmonic n_{x} may be calculated by (15). For the application, the maximum frequency variation without overlaps results in $\Delta f_{\max}\left(1\right) = \frac{1\,\mathrm{MHz}}{2\cdot 1+1} \approx 333.3\,\mathrm{kHz}$.
4) From this, the maximum achievable simultaneous reduction of peak and average may be calculated by (16). The maximum achievable reduction for the first harmonic $\Delta U_{\mathrm{Peak,dB,max}}(1\cdot 333.3\ \mathrm{kHz})$ is approximately 15.6 dB. As a reduction of only 7 dB is needed, spread spectrum can be applied successfully.
5) The desired $\Delta U_{\mathrm{Peak,dB}}(n_{\mathrm{x}}\Delta f) \leq \Delta U_{\mathrm{Peak,dB,max}}$ has to be set. By doing so, the minimal necessary frequency variation Δf can be derived from (13):

$$\Delta f(n_{\mathrm{x}}, \Delta U_{\mathrm{Peak,dB}}(n_{\mathrm{x}}\Delta f)) \approx \frac{1}{1.10\cdot n_{\mathrm{x}} T} 10^{\frac{\Delta U_{\mathrm{Peak,dB}}}{10\ \mathrm{dB}}}.$$

The reduction is chosen to 10 dB. So, a frequency variation $\Delta f(1, 10\ \mathrm{dB}) \approx 91\,\mathrm{kHz}$ results.

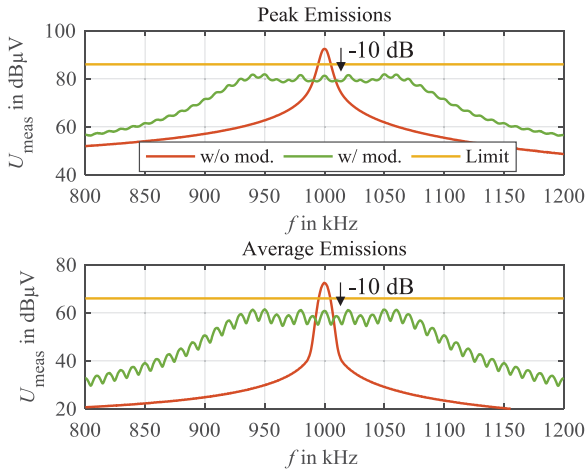

Fig. 10. Measured emissions of the burst mode signal.

The resulting spectra are depicted in Fig. 10. As calculated, both peak and average are reduced by 10 dB and are now below the limits. This example shows that the presented parametrization strategies are also applicable to sources of sporadic disturbances. As stated above, this parametrization strategy aims for a minimization of the peak emissions. In the next section, the minimization of the average emissions is discussed.

V. Minimizing Average Emissions

In this section, the influence of spread spectrum on average emissions is analyzed. As in Section IV, the optimum modulation time, the reduction for single sine waves, and the reduction for PWM signals are investigated in this section also. At the end, a systematic parametrization strategy is given. As a demonstrator, a dc-to-dc converter is used.

A. Optimum Modulation Time

To find the optimum modulation time for a minimization of the average emissions, a parameter study on the frequency

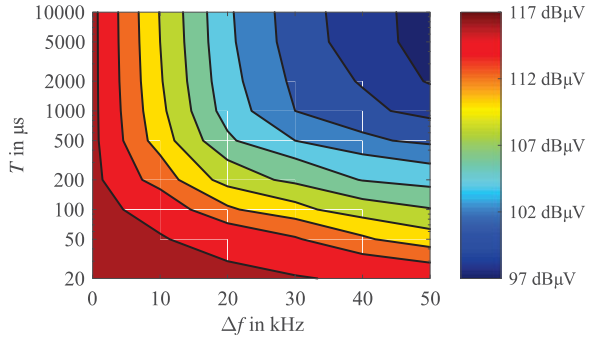

Fig. 11. Parameter study on average emissions, RBW = 9 kHz.

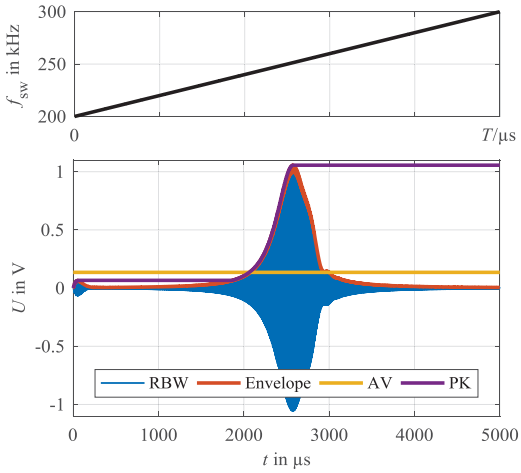

Fig. 12. Simulated signals for $T = 5$ ms and $\Delta f = 50$ kHz.

deviation Δf and the modulation time T is done. In this study, a single sine wave (representing one harmonic of a PWM signal) with an amplitude of 1 V and a nominal frequency of 250 kHz is utilized. In Fig. 11, the measured reduction of the average emissions is illustrated.

For the unmodulated case, the emissions have a level of approximately 117 dBµV. As the power of the harmonics is spread in the frequency spectrum, the average drops with an increasing frequency variation Δf. Interestingly, there is no optimum value for the modulation time T. The measured results show that long modulation times are beneficial. [22]

To understand the reduction of the average emissions, the signal is investigated in the time domain: In Fig. 12, a modulation time T of 5 ms is considered. To analyze the fundamental wave, the filter is assumed to have a center frequency of 250 kHz (making the mixer superfluous). Over a modulation period, the bandwidth filter (RBW) settles for $f_{\mathrm{sw}}\,(t) = 250$ kHz and unsettles for $f_{\mathrm{sw}}(t) \neq 250$ kHz. There is a slight overshoot increasing the peak value (PK, highest value of the envelope) to 1.06 V. Due to the modulation, the average value (AV, mean of the envelope) is reduced to 0.135 V. [22]

If there was no modulation, the amplitude at the output of the bandwidth filter would be constant at 1 V. Therefore, the envelope, peak, and average would equal 1 V. For a modulation time T close to the settling time (e.g., 100 µs), the bandwidth filter does neither settle nor unsettle. As shown in Section IV-B, this causes an equal reduction of peak and average emissions.

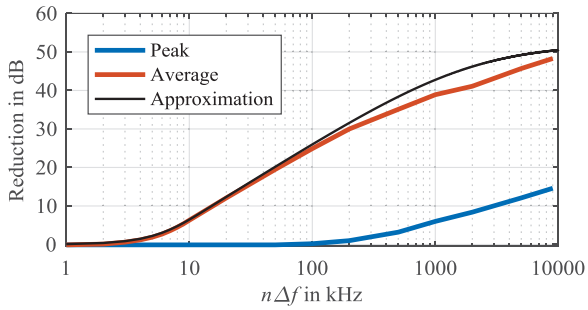

Fig. 13. Reduction of the peak and average emissions for RBW = 9 kHz, $T_{\mathrm{meas}} = 50$ ms, and $T = 5$ ms.

Nevertheless, the average emissions are not minimized for this modulation time. [22]

For implementation, a modulation time T of 5 ms is proposed due to the following reason: In electromagnetic compatibility (EMC) measurements, the measurement time must be larger than the pulse repetition time of the signal. For measurements below 30 MHz, the study in [2] prescribes minimal measurement times T_{meas} of 50 ms. To avoid a prolongation of the measurement time, the modulation time is set by

$$T \approx T_{\mathrm{meas}}/10. \tag{17}$$

In [22], it is shown that the modulation time should be much larger than the settling time of the bandwidth filter. For an ideal bandpass system with a bandwidth of BW, the settling time may be calculated by [25]

$$t_{\mathrm{settling}} \;=\; 1/\mathrm{BW}. \tag{18}$$

For a first approximation, this settling time is assumed for the input bandwidth filter (RBW). Hence, the following condition follows:

$$T \approx T_{\mathrm{meas}}/10 \gg t_{\mathrm{settling}} = 1/\mathrm{RBW}. \tag{19}$$

This condition is met by $T = 5$ ms.

B. Reduction for a Single Sine Wave

Similar to Section IV-B, the achievable reduction of the average emissions is discussed. A single sine wave $(n = 1)$ with a nominal frequency of 10 MHz is considered as a harmonic of a PWM signal. To minimize the average emissions, the modulation time T is set 5 ms. The reduction of peak and average emissions is depicted in Fig. 13.

Due to the long modulation time, the average emissions can be largely reduced. As shown in Section IV-A, this modulation time is not ideal for a reduction of the peak emissions. So, the peak emissions are only slightly reduced. Because of this, such a long modulation time should solely be applied if the average emissions must be reduced.

In the following, the reduction of the average emissions is analyzed. The basic idea is presented in Fig. 14. The RBW filter is set virtually to the nominal switching frequency of $nf_{\mathrm{sw,nom}}$. Note that there is a limited measurement dynamic between the highest measured value and the noise floor (signal-to-noise ratio, SNR). If one or multiple modulation periods are observed, the instantaneous switching frequency $nf_{\mathrm{sw}}(t)$ is repetitively in-

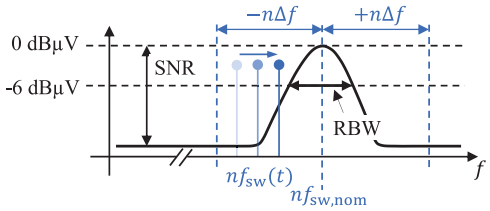

Fig. 14. Approximation of the reduction of the average emissions.

creased from $nf_{\mathrm{sw,nom}} - \Delta f$ to $nf_{\mathrm{sw,nom}} + \Delta f$. As the modulation time is relatively long, the RBW filter settles for the instantaneous switching frequencies and weights these with its transfer function. The corresponding time average delivers the average detected value.

As the bandwidth filter (RBW) is usually realized with (near)-Gaussian filters [26], the transfer function $H(f)$ is described by the Gaussian function

$$H\ (f) = a \cdot e^{-b \cdot f^2} + c\,. \tag{20}$$

The parameter c corresponds to the SNR of the device and may be calculated by

$$H\ (f \to \infty) = c = 10^{-\mathrm{SNR}/20\,\mathrm{dB}}. \tag{21}$$

In the center, the signal should be completely transmitted:

$$\begin{aligned} H\,(f\ &= 0\,\mathrm{Hz}) = a + c = 1 \\ &\Rightarrow\ a = 1 - c\,. \end{aligned} \tag{22}$$

At last, the RBW has to be considered:

$$\begin{aligned} H\ \left(f = \frac{\mathrm{RBW}}{2}\right) &= a \cdot e^{-b \cdot \left(\frac{\mathrm{RBW}}{2}\right)^2} + c \\ &= 0.5\ (\mathrel{\hat{=}} -6\ \mathrm{dB\mu V}) \\ \Rightarrow\ b &= -\left(\frac{2}{\mathrm{RBW}}\right)^2 \cdot \ln\left(\frac{0.5 - c}{a}\right). \end{aligned} \tag{23}$$

Now, the mean value is derived under the assumption that the nominal switching frequency and the center frequency of the bandwidth filter are identical:

$$\begin{aligned} \bar{\mathrm{H}}\ (n\Delta f) &= \frac{1}{2n\Delta f} \int_{-n\Delta f}^{+n\Delta f} \left(a \cdot e^{-b \cdot f^2} + c\right) df \\ \overset{\text{symmetry}}{\Rightarrow}\ \bar{\mathrm{H}}\ (n\Delta f) &= \frac{1}{n\Delta f} \int_{0}^{+n\Delta f} \left(a \cdot e^{-b \cdot f^2} + c\right) df \\ \overset{[26]}{\Rightarrow} \bar{\mathrm{H}}\ (n\Delta f) &= \frac{1}{n\Delta f} \cdot a \cdot \frac{\sqrt{\pi}}{2\sqrt{b}} \mathrm{erf}\left(\sqrt{b} \cdot n\Delta f\right) + c. \end{aligned} \tag{24}$$

So, the reduction of the AV may be described as

$$\begin{aligned} \Delta U_{\mathrm{Avg}}\ (n\Delta f) &= \bar{\mathrm{H}}^{-1}\ (n\Delta f) \\ &\Rightarrow \Delta U_{\mathrm{Avg,dB}}\ (n\Delta f) \end{aligned} \tag{25}$$

$$= 20\,\mathrm{dB}\ \log_{10}\left\{\left(\frac{a \cdot \sqrt{\pi}}{2\sqrt{b} \cdot n\Delta f} \mathrm{erf}\left(\sqrt{b} \cdot n\Delta f\right) + c\right)^{-1}\right\}. \tag{26}$$

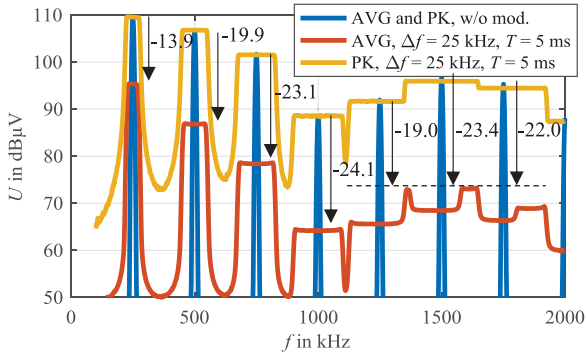

Fig. 15. Exemplary spectra of PWM signals, $f_{\mathrm{sw,nom}} = 250\,\mathrm{kHz}$, $d = 77\,\%$.

TABLE II
AVERAGE REDUCTIONS IN THE EXEMPLARY SPECTRA

Harmonic	1	2	3	4	5	6	7
Δf/kHz	25	50	75	100	125	150	175
$\Delta U_{\mathrm{Avg,dB,meas}}$/dB	13.9	19.9	23.1	24.1	19.0	23.4	22.0
$\Delta U_{\mathrm{Avg,dB,calc}}$/dB	14.3	20.2	23.6	26.0	27.8	29.3	30.5

This approximation is found in Fig. 13 and proves itself viable (the SNR of the system is approximated to 52 dB).

C. Reduction for a PWM Signal

Next, exemplary spectra of a PWM signal (see Fig. 15) are discussed. Similar to Section IV-C, the first overlap of the harmonics occurs for

$$n_{\mathrm{ovlp}} = \mathrm{ceil}\left(\frac{f_{\mathrm{sw,nom}}}{2\Delta f} - \frac{1}{2}\right). \tag{27}$$

In this case, there is the first overlap for the fifth harmonic. For the peak emissions, this has no further impact. As discussed before, the peak emissions are only marginally reduced. In Table II, a comparison between the calculated and measured average reductions is presented. Similar to Section IV-C, the highest reduction is achieved for the last harmonic (fourth) before an overlap occurs.

Again, the maximum frequency variation for a specific harmonic (without overlap) may be calculated by

$$\Delta f_{\max}\ (n_{\mathrm{x}}) = \frac{f_{\mathrm{sw,nom}}}{2n_{\mathrm{x}} + 1}. \tag{28}$$

With (26), the maximum achievable reduction of the average emissions $\Delta U_{\mathrm{Avg,dB,max}}(n_{\mathrm{x}}\Delta f_{\max}(n_{\mathrm{x}}))$ may be determined.

D. Systematic Selection of Spread Spectrum Parameters

In this section, the theoretical results are integrated to a systematic parametrization strategy in order to fulfill specific requirements. This procedure is applicable if only the average emissions must be reduced. If both peak and average emissions must be reduced, the parametrization strategy of Section IV-D must be applied.

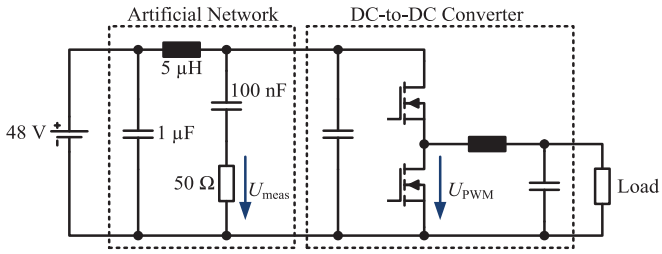

Fig. 16. Schematic diagram of the measurement setup.

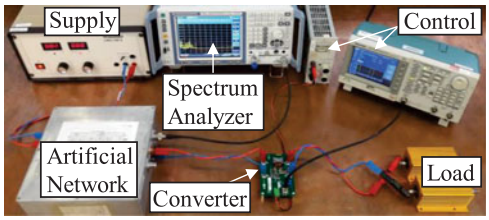

Fig. 17. Photograph of the measurement setup.

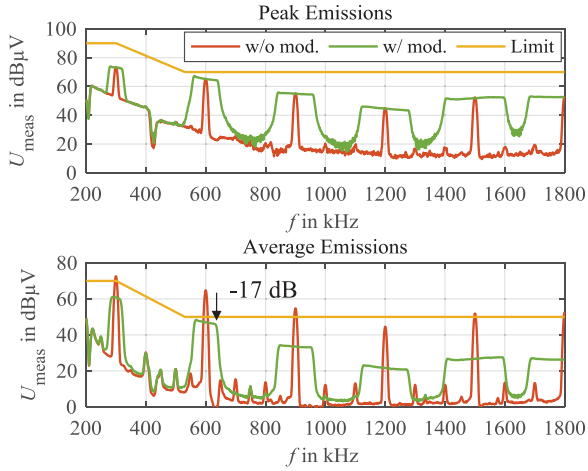

Fig. 18. Measured emissions of the dc-to-dc converter.

As an example, the GaN-based evaluation board GS61008P-EVBBK is used as a dc-to-dc converter (see Figs. 16 and 17). The converter connects the voltage levels 48 and 12 V and operates at a nominal switching frequency of 300 kHz. As the used GaN-HEMTs are conductive for reversed polarity, antiparallel freewheeling diodes are not needed. Low- and high-side transistors are turned on and off alternately and produce a PWM signal–the source of EMI. The switching pattern is controlled by an arbitrary waveform generator. Hence, spread spectrum can easily be studied. AM broadcasting (RBW of 9 kHz) with its class 3 limit [2] is investigated. The resulting spectra are depicted in Fig. 18. For the unmodulated case, the peak emissions fulfill the given limits. However, multiple harmonics violate the limit for the average emissions.

The proposed parametrization strategy for spread spectrum consists of the following steps.

1) The modulation time is set according to (19). As AM is considered, a measurement time of 50 ms and a RBW of 9 kHz are required. From these data, a modulation time T of 5 ms is recommended.
2) Next, the critical harmonic n_x has to be identified. If there are multiple critical harmonics, note that every harmonic before n_x is reduced less. All harmonics after n_x are still reduced but not as much as the harmonic n_x. In the example, the second harmonic ($n_\mathrm{x} = 2$) at 600 kHz with its level of 65 dBµV is most critical. Its value is 15 dB above the limit.
3) Now, the maximum frequency variation without overlaps in the harmonic $n_\mathrm{x} = 2$ may be calculated by (28): $\Delta f_\mathrm{max}(2) = \frac{300\,\mathrm{kHz}}{2\cdot 2+1} \approx 60\,\mathrm{kHz}$.
4) From this, the maximum achievable reduction for the harmonic n_x may be determined by (26): $\Delta U_\mathrm{Avg,dB,max}(2 \cdot 60\,\mathrm{kHz} = 120\,\mathrm{kHz}) \approx 26\,\mathrm{dB}$. Alternatively, a graphical approach using Fig. 13 is proposed. Note that (26) has to be plotted again for other values of SNR and RBW. The value of 26 dB is much higher than the required reduction of 15 dB. So, spread spectrum can be applied successfully.
5) Next, the desired $\Delta U_\mathrm{Avg,dB}(n_\mathrm{x}\Delta f) \leq \Delta U_\mathrm{Avg,dB,max}$ is chosen to 17 dB. By doing so, the lowest frequency variation Δf can be found that meets the requirements. It is recommended to use Fig. 13 to determine $2\Delta f(2, 17\,\mathrm{dB}) \approx 40\,\mathrm{kHz}$. Therefore, a Δf of approximately 20 kHz results.

So, spread spectrum is applied with the parameters $T = 5$ ms and $\Delta f = 20\,\mathrm{kHz}$. The result can be found in Fig. 18. The average of the critical harmonic is successfully reduced by 17 dB. As explained beforehand, the lower and higher harmonics are reduced as well. By the application of spread spectrum, the average emissions meet the EMI requirements of the system. As analyzed in Section V-A, the peak emissions are mostly unchanged.

VI. Quasi-Peak Emissions

Besides the peak and average emissions, the quasi-peak emissions are also an important measure that take the repetition rate of the disturbances into account. For high repetition rates, both detectors achieve similar results. For low repetition rates, the quasi-peak detector finds a lower value than the peak detector.

For spread spectrum, the modulation time T defines the repetition rate. To evaluate for which modulation times T the peak and quasi-peak detectors achieve similar results, measurements were performed. In this study, a single sine wave with a nominal frequency of 1 MHz and a frequency variation Δf of 100 kHz is applied. Again, an RBW of 9 kHz is used. The amplitude of the unmodulated signal is 1 V that equals 117 dBµV for the RMS value. In the measurement, the modulation time T is varied over a wide range. The result is depicted in Fig. 19. It can be seen that peak and quasi-peak are similar for low modulation times up to approximately 50 ms. For modulation times above 50 ms, the repetition rate is so low that the quasi-peak emissions drop in comparison to the peak emissions.

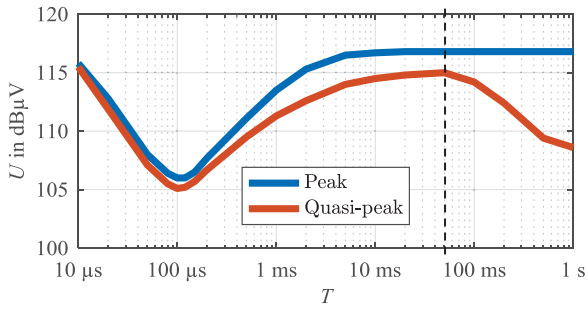

Fig. 19. Comparison of peak and quasi-peak emissions.

In this paper, modulation times below 10 ms are discussed. So, in regard to the quasi-peak detector, the repetition time is rather high. Therefore, the analysis, results, and conclusions for the peak detector can be transferred to the quasi-peak detector.

VII. Conclusion

In this contribution, peak and average emissions have been analyzed if spread spectrum is applied. This analysis has shown that peak and average emissions are affected differently by spread spectrum.

1) To minimize the peak emissions, a modulation time slightly higher than 1/RBW is needed.
2) To minimize the average emissions, the modulation time should be chosen much higher.

The reduction of the peak and average emissions has been analyzed and mathematically described. It has been shown that overlaps of spread harmonics limit the effectivity of spread spectrum at higher harmonics and/or higher frequency variations.

These results have been integrated to systematic parametrization strategies that help with the adjustment of the parameters of spread spectrum in order to fulfill specific EMI requirements.

The effectivity of spread spectrum and the derived parametrization strategies has been demonstrated on a dc-to-dc converter and a burst mode signal. Furthermore, it is shown that peak and quasi-peak emissions behave similarly for the considered modulation times.

References

[1] *ECE R10 No. 10—Electromagnetic Compatibility, Rev. 5*, 2014.
[2] *CISPR 25—Vehicles, Boats and Internal Combustion Engines—Radio Disturbance Characteristics—Limits and Methods of Measurement for the Protection of On-Board Receivers*, 2015.
[3] F. Lin and D. Y. Chen, "Reduction of power supply EMI emission by switching frequency modulation," *IEEE Trans. Power Electron.*, vol. 9, no. 1, pp. 132–137, Jan. 1994.
[4] K. B. Hardin, J. T. Fessler, and D. R. Bush, "Spread spectrum clock generation for the reduction of radiated emissions," in *Proc. IEEE Int. Symp. Electromagn. Compat.*, Chicago, IL, USA, Aug. 22–26, 1994, pp. 227–231.
[5] F. Pareschi, R. Rovatti, and G. Setti, "EMI reduction via spread spectrum in DC/DC converters: State of the art, optimization, and tradeoffs," *IEEE Access*, vol. 3, pp. 2857–2874, Dec. 2015.
[6] D. Stepins, "Conducted EMI of switching frequency modulated boost converter," *Elect. Control Commun. Eng.*, vol. 3, no. 1, pp. 12–18, Sep. 2013.
[7] B. Weiss *et al.*, "Switching frequency modulation for GaN-based power converters," in *Proc. IEEE Energy Convers. Congr. Expo.*, Montreal, QC, Canada, Sep. 20–24, 2015, pp. 4361–4366.
[8] S. Callegari, R. Rovatti, and G. Setti, "Spectral properties of chaos-based FM signals: Theory and simulation results," *IEEE Trans. Circuits Syst. I, Fundam. Theory Appl.*, vol. 50, no. 1, pp. 3–15, Jan. 2003.
[9] F. Pareschi, G. Setti, R. Rovatti, and G. Frattini, "Short-term optimized spread spectrum clock generator for EMI reduction in switching DC/DC converters," *IEEE Trans. Circuits Syst. I, Reg. Papers*, vol. 61, no. 6, pp. 3044–3053, Oct. 2014.
[10] J. Jankovskis, D. Stepins, and D. Pikulin, "Efficiency of PFC operating in spread spectrum mode for EMI reduction," *Elektron. Elektrotech.*, vol. 103, no. 7, pp. 13–16, 2010.
[11] J. Jankovskis, D. Stepins, and N. Ponomarenko, "Effects of spread spectrum on output filter of buck converter," *Elektron. Elektrotech.*, vol. 19, no. 7, pp. 45–48, 2013.
[12] J. Mon, D. González, C. Gautier, D. Labrousse, and F. Costa, "Coupled interleaved multicellular parallel converters operated under switching frequency modulation," in *Proc. 2014 16th Eur. Conf. Power Electron. Appl.*, Lappeenranta, Finland, Aug. 26–28, 2014, pp. 1–7.
[13] J. Mon, J. Gago, D. González, J. Balcells, R. Fernández, and I. Gil, "A new switching frequency modulation scheme for EMI reduction in multiconverter topology," in *Proc. 13th Eur. Conf. Power Electron. Appl.*, Barcelona, Spain, Sep. 8–10, 2009, pp. 1–8.
[14] J. Mon, D. González, J. Gago, J. Balcells, R. Fernández, and I. Gil, "Contribution to conducted EMI reduction in multiconverter topology," in *Proc. 2009 35th Annu. Conf. IEEE Ind. Electron.*, Porto, Portugal, Nov. 3–5, 2009, pp. 4086–4091.
[15] W. Cho, E. J. Powers, and S. Santoso, "Low and high frequency harmonic reduction in a PWM inverter using dithered sigma-delta modulation," in *Proc. 10th Int. Conf. Inf. Sci. Signal Process. Appl.*, Kuala Lumpur, Malaysia, May 10–13, 2010, pp. 440–443.
[16] K. Inoue, K. Kusaka, and J. Itoh, "Reduction on radiation noise level for inductive power transfer systems with spread spectrum focusing on combined impedance of coils and capacitors," in *Proc. IEEE Energy Convers. Congr. Expo.*, Milwaukee, WI, USA, Sep. 18–22, 2016, pp. 1–8.
[17] A. C. Binoj Kumar and G. Narayanan, "Variable-switching frequency PWM technique for induction motor drive to spread acoustic noise spectrum with reduced current ripple," *IEEE Trans. Ind. Appl.*, vol. 52, no. 5, pp. 3927–3938, Sep./Oct. 2016.
[18] B. Deutschmann, B. Auinger, and G. Winkler, "Spread spectrum parameter optimization to suppress certain frequency spectral components," in *Proc. 11th Int. Workshop Electromagn. Compat. Integr. Circuits*, St. Petersburg, Russia, Jul. 4–8, 2017, pp. 39–44.
[19] D. Kesling and H. Skinner, "New spread spectrum clocking techniques for improved compatibility with cellular and wireless subsystems," in *Proc. IEEE Int. Symp. Electromagn. Compat.*, Raleigh, NC, USA, Aug. 4–8, 2014, pp. 177–180.
[20] T. Karaca and M. Auer, "Characterization of EMI-reducing spread-spectrum techniques for class-D audio amplifiers," in *Proc. Asia-Pacific Int. Symp. Electromagn. Compat.*, Shenzhen, China, May 17–21, 2016, pp. 791–793.
[21] H. G. Skinner and K. P. Slattery, "Why spread spectrum clocking of computing devices is not cheating," in *Proc. IEEE Int. Symp. Electromagn. Compat.*, Montreal, QC, Canada, Aug. 13–17, 2001, pp. 537–540.
[22] A. Bendicks, H. Haverland, S. Frei, N. Hees, and M. Wiegand, "Application of spread spectrum techniques for the reduction of disturbances of automotive power electronic converters," in *Proc. Int. Conf. Elect. Electron. Syst. Hybrid Elect. Veh. Elect. Energy Manage.*, Bamberg, Germany, May 17–18, 2017.
[23] H. S. Black, *Modulation Theory*. New York, NY, USA: Van Nostrand, 1953.
[24] J. R. Klauder, A. C. Price, S. Darlington, and W. J. Albersheim, "The theory and design of chip radars," *Bell Syst. Tech. J.*, vol. 39, no. 4, pp. 745–808, Jul. 1960.
[25] J.-R. Ohm and H. D. Lüke, *Signalübertragung*, 11th ed. Heidelberg, Germany: Springer, 2010.
[26] *Spectrum Analysis Basics—Application Note 150*, Agilent, Santa Clara, CA, USA, Nov. 2016.
[27] I. N. Bronshtein, K. A. Semendyayev, M. Mühlig, and G. Musiol, *Handbook of Mathematics*, 6th ed. Berlin, Germany: Springer, 2015.
[28] C. R. Paul, *Introduction to Electromagnetic Compatibility*, 2nd ed. Hoboken, NJ, USA: Wiley, 2006.

Andreas Bendicks (S'17) received the B.S. and M.S. degrees in electrical engineering from RWTH Aachen University, Aachen, Germany, in 2013 and 2016, respectively.

He is currently a Research Assistant with the On-Board Systems Lab, TU Dortmund University, Dortmund, Germany. His field of research covers active methods to improve the electromagnetic compatibility of power electronic converters in automotive applications. His research interests include electromagnetic interference (EMI)-optimized control schemes and active EMI cancellation.

Stephan Frei (M'97–SM'13) received the Dipl.-Ing. degree in electrical engineering from Berlin University of Technology, Berlin, Germany, in 1995, where he received the Ph.D. degree in electrical engineering from the Institute of Electrical Power Engineering in 1999.

Between 1995 and 1999, he was a Research Assistant of electromagnetic compatibility (EMC) with the Institute of Electrical Power Engineering, Berlin University of Technology. Between 1999 and 2005, he was with the automaker AUDI AG in the Development Department, where he developed and introduced new methods for the computation of EMC, antennas and signal integrity (SI) in vehicles. Furthermore, he was responsible for the EMC release process of several vehicles and international standardization. In 2006, he became a Professor for vehicular electronics with TU Dortmund University, Dortmund, Germany, where his research interests include EMC, SI, computational methods, and vehicle power supply systems. He is the author of more than 180 papers.

Dr. Frei served as the Distinguished Lecturer for the IEEE EMC Society from 2008 to 2009. He is currently the Vice Dean of the Faculty for Electrical Engineering and Information Technology, TU Dortmund University.

Norbert Hees received the Dipl.-Ing. degree in electrical engineering from the University of Siegen, Siegen, Germany, in 1996.

After several stages in development departments in the electrical and medical devices industries, he joined Leopold KOSTAL GmbH & Co. KG, Lüdenscheid, Germany, in 2002, where he was a Software Engineer and a Project Manager in the development of electrical drives applications until 2011. From 2011, he is responsible for the advanced development of power electronics in the KOSTAL Automotive Electrical Systems business domain.

Marc Wiegand received the Dipl.-Ing. degree in electronic engineering from the University of Dortmund, Dortmund, Germany, in 1999.

He started his career as a Hardware Engineer with Delphi-Megamos, Wiehl-Bomig. He joined Leopold KOSTAL GmbH & Co. KG in 2002 as electromagnetic compatibility (EMC)-Engineer in Lüdenscheid. From 2011 to 2015, he was involved in advanced engineering for inductive charging systems and other future products for the KOSTAL Group. From 2015, he is responsible for EMC for power electronics and control units at KOSTAL, Dortmund.